ORIGINAL ARTICLE

Hsueh-Yu Lu

A method to estimate hydraulic conductivity from bulk geochemical compositions

H.-Y. Lu
Department of Earth and Environmental
Sciences, National Chung Cheng
University, 168, University Road,
Min-Hsiung Chia-Yi,
Chung Cheng, Taiwan
E-mail: seishei@eq.ccu.edu.tw
Tel.: +886-5-2720411
Fax: +886-5-2720807

Abstract A new method has been developed to estimate the hydraulic conductivity in unconsolidated aquifers. The method uses bulk geochemical compositions correlated with hydraulic conductivities measured by pumping tests. The concept is based on a general rule that hydraulic conductivity is principally controlled by grain-size distribution and particle shape, both of which relate to mineralogical composition. Using a MINLITH algorithm, normative mineralogical compositions can be derived from bulk geochemical compositions economically and expediently, and then correlated to the hydraulic conductivity determined by pumping tests in the field. In this study, 202 sediment samples from nine unconsolidated aquifers were analyzed by X-ray fluorescence.

Although hydraulic conductivity does not show a definite relationship with geochemical compositions, it does demonstrate a linear logarithmic equation to the content of normative earthy minerals. However, linear regressed equations should not be applied to aquifers composed of medium to coarse sand and gravel sizes due to interference from lithic fragments. In addition, this equation tends to overestimate hydraulic conductivity possibly because the effect of compaction is ignored in this study.

Keywords Hydraulic conductivity · Bulk geochemical composition · Normative mineralogical composition · X-ray fluorescence analysis

Introduction

Hydraulic conductivity is one of the most important properties of a hydrogeological system. It is essential both for modeling groundwater flow and solute transport in aquifers. A large number of measurement methods have been developed to determine hydraulic conductivity. An in situ pumping test has proven to be the most reliable method for determining hydraulic conductivity. Such testing can also usually identify the existence of secondary fractures serving as preferential flow paths for groundwater flow. In the last decade, some advanced in situ approaches have been developed for revealing information about vertical variations in hydraulic conductivity on a single-well basis. These include slug test in direct-push drilling (e.g., Hinsby et al. 1992; Butler et al. 2002) and dipole-flow test (e.g., Kabala 1993; Zlotnik and Ledder 1996). The direct-push drilling technology uses hydraulic pressure to advance sampling devices and analytical sensors into the subsurface. Samples of water, soil and gas vapor and geophysical information can undisturbedly be collected from up to 30 m beneath the surface in unconsolidated deposits. Instead of an average value of aquifer hydraulic conductivity, a vertical profile of hydraulic conductivities can be determined by conducting pump tests or slug tests. The dipole-flow test uses a three-packer tool to build up a discrete-interval isolation

system for generating recirculatory flow to evaluate aquifer properties. Because the packer system can be defined and controlled as expected, it is useful for characterization of vertical aquifer heterogeneity. However, application of these methods, especially on a multi-well basis, is expensive, time-consuming and invasive.

An alternative method of field aquifer testing is laboratory determination of hydraulic conductivity while a core sample is available. Hydraulic conductivity can be measured directly with permeameters under the flow regime of Darcy's law. Laboratory measurements are economical and time saving but laboratory samples are extremely small compared to the aquifer as a whole and some degree of disturbance always accompanies the collection of samples. Frequently, core samples need to be fully remodeled for those in bad shape or to prevent fractures from dominating the flow regime. For these reasons, estimates obtained from laboratory work may not be sufficient to completely describe the hydraulic properties of an aquifer.

Theoretically, permeability can be measured only when a porous medium transmits a liquid under a potential gradient. However, there are additional factors governing permeability such as some types of geophysical logs, and soil properties, especially grain size. For example, a local-area empirical relationship between natural-gamma-log intensity and permeability was demonstrated by Rabe (1957) and Gaur and Singh (1965). Croft (1971) showed that the relationship between permeability and formation-resistivity factor obtained from electric logs was in reasonable agreement with those obtained by other methods. It should be noted that geophysical logs are not only related to aquifer lithology including porosity, grain-size distribution, particle shape, particle orientation and type of cementation, but also to fluid properties and borehole conditions. Namely, water quality should also be assessed to eliminate interference. Although fluid properties have much less effect on nuclear logs (unless the fluid is contaminated by radioactive elements), borehole conditions, such as borehole diameter and detector position, may introduce errors in measuring radioactive intensity while radioactive rays emitted from aquifer sediments pass through different travel lengths. In addition, the recording-time constant and logging speed ought be considered when interpreting nuclear logs. For all these reasons, geophysical-log records represent relative measurements and consequently need to be carefully calibrated in advance for quantitative interpretation.

Grain-size distribution is another important soil property frequently correlated with hydraulic conductivity (e.g., Hazen 1911; Pryor 1973). Shepherd (1989) summarizes the empirical relations with the expression:

$$K = aD^b \tag{1}$$

where K is the hydraulic conductivity in m/s, D is the effective grain size in mm and a and b are constants depending on the soil properties. These constants integrate all other factors that may affect aquifer hydraulic property. In general, effective grain size is designated as a grain size that is 10% finer by weight (D_{10}). It suggests permeability to be controlled by the finer grain sizes in soils (Hazen 1911).

In this study, a new method has been developed to estimate aquifer hydraulic conductivity using bulk geochemical compositions. The concept is based on a general rule that hydraulic conductivity is principally controlled by grain-size distribution and particle shape. Both of which relate to mineralogical composition. This rule holds reasonably for mature soils containing minor amounts of lithic fragments. In general, a mature soil is mainly composed of tectosilicate and phyllosilicate minerals. The tectosilicates, including quartz and feldspar, are of phases directly from their parent rocks. Compared to phyllosilicate minerals, the crystals of tectosilicates are generally granular and larger in size establishing aquifers that have grain-supporting frameworks with naturally interconnected pore spaces and higher permeability. In contrast, phyllosilicates, of which clay minerals form a major subgroup, are most probably formed from the weathered products of parent rocks or as a result of transformation from other clay minerals during diagenesis or metamorphism. These clay minerals have very thin sheet-like crystal habit due to a layered structure composed of shared octahedral and tetrahedral sheets. Accordingly, the word "clay" is also used to refer to particle size in soil. The International Society of Soil Science defines "clay" as being a soil particle of rock or mineral origin less than 0.002 mm in diameter (Davis and Bennett 1927), whereas sedimentologists classify particles smaller than 0.004 mm (1/256 mm) as clay (Wentworth 1922). Soil composed of such fine-grained, sheet-like phyllosilicates will have a matrix-supporting rather than grain-supporting structure. The fine nature of clay particles clog the pore spaces dramatically reducing aquifer permeability. In addition, vertical permeability is suppressed by a factor of 10 due to the sheet-like orientation of particles during burial compaction. Utilizing mineralogical composition in this manner, it is possible to statistically derive aquifer hydraulic conductivity.

In practice, optical identification and the counting of minerals corresponding to points in a grid pattern are frequently used to determine the mineralogical assemblage. Such methods have intrinsic drawbacks such as point counting being labor-intensive work requiring experienced operators. Measurement of mineralogical assemblage can also be performed by scanning electron

microscopy with energy dispersive X-ray analysis (SEM-EDXA) interfaced to an image analyser. SEM-EDXA relies on less-specialized experience; however, many rock-forming minerals have similar or overlapping gray levels. Therefore, additional discrimination of minerals has to be made. Another economical and efficient method involves X-ray diffraction to identify minerals and quantify their abundances based on peak intensities. However, it is semi-quantitative because the peak intensity of selected wavelengths usually has no linear relationship with mineral abundance.

In this study, a mathematical algorithm was employed to estimate the mineralogical composition, called norm, which was applied originally to igneous rocks in the form of the CIPW norm proposed by four petrologists, Cross, Iddings, Pirsson and Washington (Cross et al. 1902). This normative mineralogical composition is directly calculated from bulk geochemical analyses. There are several computer programs designed to apply exclusively to sedimentary rocks (Cohen and Ward 1991; Merodio et al. 1992; Rosena et al. 2004), and some other general-purpose algorithms that consider only mass conservation for selected elements that can be applied to sedimentary rock (Currie 1991; de Caritat et al. 1994; Paktunc 1998). Consequently, in this study, normative mineralogical compositions will be correlated to hydraulic conductivities measured by pumping tests in the field.

Sampled aquifers

In order to select qualified aquifers for subsequent analysis of hydraulic conductivities, drawdown versus time data in pumping tests have to be carefully examined to ensure accuracy. Drawdown–time semi-log plots of nonlinear fit or low correlation coefficient (possibly involving interference from other pumping wells or bad well performance) were ruled out at first. In addition, aquifers composed of medium to coarse sand and gravel were also excluded to ensure soil free of lithic fragments, thereby avoiding the MINLITH algorithm giving an incorrect normative mineralogical assemblage. However, it was found that most monitoring wells were installed at sites of relative high permeability likely to contain substantial lithic fragments. This meant that only a few monitoring wells were suitable for use in this study. Naturally, core samples must also be available. According to the aforementioned constraints, nine unconsolidated aquifers from four different sites (Fig. 1) were selected from the national Taiwan Groundwater Monitoring Network (TGMN). The TGMN was initiated in 1992 for fundamental investigation of groundwater resources in Taiwan. This project installs 15–25 new wells each year, and presently has over 900 monitoring wells Taiwan wide.

Of the four sample sites, three (sites 1–3) are located in southwestern Taiwan. In this area, the aquifers were deposited mostly in environments of Holocene continental shelf to littoral sea. Although fluvial sedimentation developed during the last glacial period, 18,000 years ago, coarse sediments are still rare due to an absence of sandstone in source areas and the dominance of shale and mudstone. Hence a confluence of environmental circumstances meant that most of the samples collected for this study were sourced from this area owing to the appropriate relationship between mineralogical composition and hydraulic conductivity. One additional site (site 4) was sampled in the coastal area of mid-northern Taiwan. Aquifers in this area are mainly composed of Pleistocene sediments; and the Holocene aquifers are restricted to creek valleys and narrow coastal plains. Most of the aquifers consist of coarse alluvial deposits except for the one selected for this study, being far away from any creek channel.

The sites were drilled using hydraulic rotary techniques and the cores were retrieved using a 4-in. diameter core barrel. The cores were split longitudinally by a diamond saw into two halves, with one half taken for sampling purposes and the other half being retained. Before sampling, drilling mud should be removed from the split-core surface using a clean, dry knife to eliminate contamination on chemical compositions. A total of 202 samples, 5–10 cm long, were collected at depths based on changes in grain size. The split cores were also described based on soil-grain size as shown in the stratigraphic columns (Fig. 2). It is obvious that most of the monitoring wells of the selected sites were installed in aquifers composed of fine sands. Aquifers with coarser sediments are very limited. However, three additional medium-sand aquifers, including the first aquifer of site 2, the first aquifer of site 3 and the second aquifer of site 4, were also sampled for demonstrating the effect of rock fragments on bulk geochemical compositions and normative mineralogical compositions.

Analytical methods

X-ray fluorescence (XRF) analysis is one of the most widely used routine instrumental methods of elemental analysis of geological materials. Compared to digestion for wet-chemical analysis, XRF analysis is highly reliable with simple sample preparation procedures; these are generally automated. This makes such analysis eminently suitable for determining the bulk geochemical compositions of major elements in the over 200 sediment samples of this study.

To produce a glass disk for subsequent XRF analysis, the entire sample was crushed and ground into a powder with a particle size finer than 100 μm. The sample powder and anhydrous lithium tetraborate ($Li_2B_4O_7$)

Fig. 1 Map of Taiwan showing the four locations of sampled aquifers. *Solid circles* show locations of sampling sites
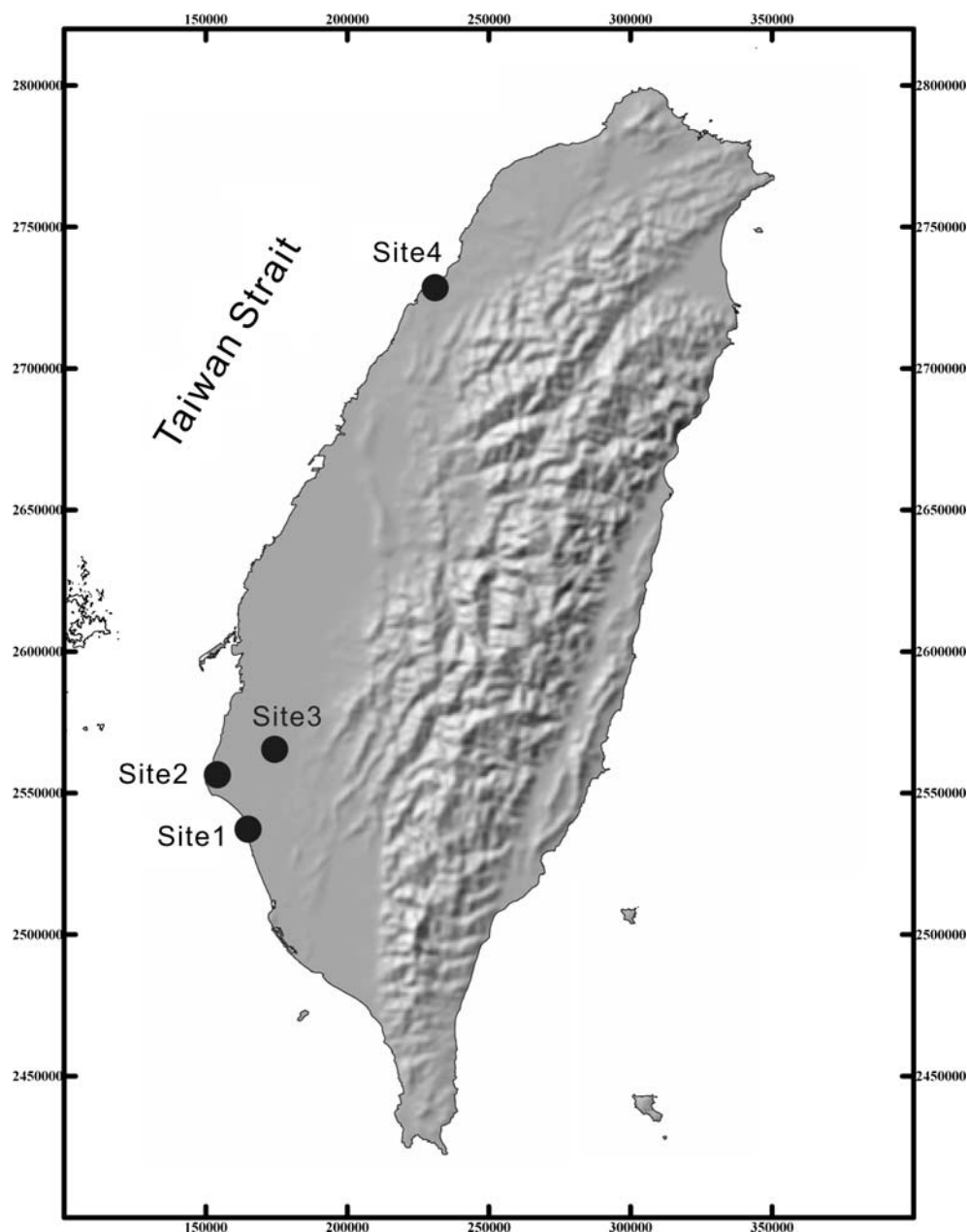
used as flux were dried at 110°C for 24 h, and then cooled down to room temperature in an electronic drying cabinet. Dried sample powders of 0.4 g were weighed to an accuracy of 0.0001 g on an analytical balance, and homogenized in 4 ± 0.0001 g of anhydrous lithium tetraborate. The mixture was then transported to a 5% gold/95% platinum crucible and fused into a glass disk in an automatic fusion machine. Finally, the fused glass disks were analyzed for ten major elements reported as oxides, including SiO_2, TiO_2, Al_2O_3, Fe_2O_3, MnO, MgO, CaO, Na_2O, K_2O and P_2O_5, by Rigaku RIX2000 spectrometer. Amounts other than the ten major oxides were roughly estimated as loss on ignition (LOI).

Based on the resultant chemical compositions from XRF analysis, normative mineralogical compositions were subsequently calculated by a mathematical algorithm, MINLITH computer code (Rosena et al. 2004). The mineralogical assemblage in a sedimentary rock is seldom likely to reach a mineralogical equilibrium state, as might be expected in a crystallized igneous material. However, some other significant statistical regularities are available to be employed in quantitatively interpreting the effects of weathering, sedimentation and diagenesis on mineralogical compositions. MINLITH uses these experience-based regularities to estimate the most likely mineralogical assemblage from bulk geo-
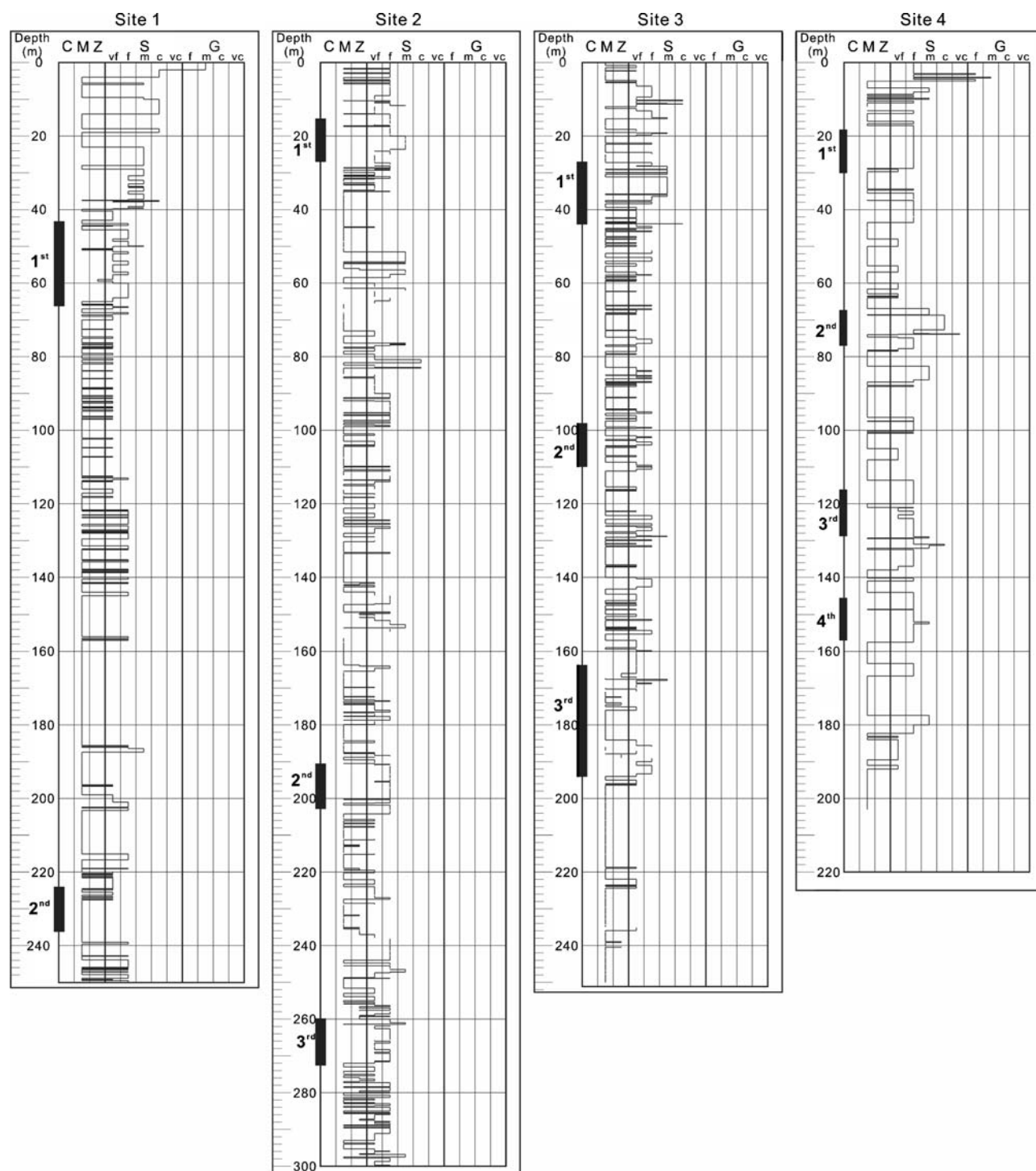
Fig. 2 Stratigraphic columns of nine sampled aquifers from the four sites. The *thick line* by the side of the depth ruler portrays the range of well screens. Grain size of C, M, Z, M and G represent clay, mud, silt, sand and gravel, respectively. Descriptors: *vf*, *f*, *m*, *c* and *vc* represent very fine, fine, medium, coarse and very coarse, respectively

chemical compositions. There is no need to change parameters or select options, and the answer is unique. It is economical, time-saving and therefore utilized in this study. Nevertheless, validation of MINLITH does need to be carefully examined.

Results and discussion

Bulk chemical compositions

The results of the XRF measurements for the 202 sediment samples show that sample SG29 from site 1 contains extraordinarily high concentrations of Fe_2O_3 (21.66%) and MnO (3.25%); this may have been the result of iron nodules formed during diagenesis. Excluding sample SG29, the major elements present the following compositional range: SiO_2 = 55.33–90.33%, TiO_2 = 0.28–1.11%, Al_2O_3 = 4.30–20.85%, Fe_2O_3 = 1.38–10.43%, MnO = 0.01–0.53%, MgO = 0.19–2.82%, CaO = 0.19–10.64%, Na_2O = 0.01–2.45%, K_2O = 1.24–3.86%, P_2O_5 = 0.04–1.61%, LOI = 1.07–14.18%. The relationships among major element compositions can be further examined (Fig. 3).

1. A negative correlation between Al_2O_3 and SiO_2 (r^2 = 0.948) indicates that the sediments are principally composed of minerals enriched with Al_2O_3 or SiO_2 (Fig. 3a). Samples deviating from the regression line, including HB11-13, HB44-45, HB48-50 and SG33, have lower concentrations of Al_2O_3 or SiO_2 due to considerable amounts of calcareous fossil fragments.
2. A high positive correlation between K_2O and Al_2O_3 (r^2 = 0.937) shows that illite is the most dominant clay mineral in the samples (Fig. 3b).
3. A random distribution in the plots of CaO and Na_2O versus Al_2O_3 demonstrates that CaO and Na_2O come from multiple sources (Fig. 3c, d).
4. A positive correlation between Fe_2O_3 and Al_2O_3 (r^2 = 0.894) indicates that Fe_2O_3 in the sediments occurs mostly in the illite (Fig. 3e). Samples with higher iron oxides, including SG33, ZY22, HB01, HB03, HB44 and HB48, may contain substantial iron nodules, and are excluded from regression analysis.
5. As shown in Fig. 3f, the concentrations of MnO in the samples are too low to obtain a high correlation with Al_2O_3 (r^2 = 0.426).
6. That illite and chlorite are the dominant clay minerals in the sampled sediments makes a positive correlation between MgO and Al_2O_3 (Fig. 3g). However, MgO may come from other sources, e.g., dolomite, montmorillonite and serpentine, to accomplish a lower correlation coefficient (r^2 = 0.801).
7. A high positive correlation between TiO_2 and Al_2O_3 (r^2 = 0.921) indicate Al and Ti as being stable residual elements with a relationship inherited from their parent rocks (Fig. 3h).

As the above discussion reveals, aluminosilicates and quartz are the most dominant mineral phases, the exceptions being mostly the result of calcareous fossils or iron nodules. High correlation between Al_2O_3 versus K_2O, MgO and TiO_2 suggests that these samples are

▶

Fig. 3 Concentrations of selected major elements in sampled sediments are plotted against their concentrations of Al_2O_3. The labeled data are samples deviating from the regression line, and therefore not included for regression analysis

strongly weathered (Holail and Moghazi 1998). All these evidences support most of the samples being from mature soil samples, i.e., they are almost free of unstable minerals such as pyroxenes and olivines. Hence, these samples are suitable for subsequent analysis with the MINLITH algorithm, which does not allow for any unstable mineral phases during the calculation of normative mineralogical compositions.

Normative mineralogical compositions

The normative minerals used by the MINLITH algorithm are listed in Table 1 (Rosena et al. 2004). Based on mass conservation for each element from all presumed normative minerals, the normative mineralogical compositions were calculated. The results show that quartz is the most dominant mineral phase ranging from 21.4 to 83.1%. However, seven normative minerals, carbon, fluorite, gibbsite, gypsum, halite, magnesite and pyrite, were not detected in any sample because elements of C, F, S and Cl were not analyzed.

To evaluate the validation of the MINLITH algorithm, the relationship between phyllosilicates (illite, montmorillonite, chlorite and kaolinite) and tectosilicates (albite, anorthite, orthoclase and quartz) is shown in Fig. 4. The high negative correlation (r^2 = 0.982) demonstrates that phyllosilicates and tectosilicates are not only the most dominant minerals in the samples but also complementary to each other. The labeled samples are consistent with those in Fig. 3a, resulting from the presence of calcareous fossils or iron nodules. In addition, Fig. 5 shows a familiar trend that coarser the sediments the lower the content of phyllosilicates. Therefore, the normative mineral content derived from the MINLITH algorithm does not violate the interpretations based on major element compositions, and thus the results of the algorithm are able to represent quantitatively significant components of mineralogical assemblage.

It is important that there are still some samples against the general trend. As shown in Fig. 5, the first aquifer in site 2 and the first aquifer in site 3 are mainly composed of medium sands but their normative pelitic minerals are almost 30% higher than those of the fine-sand aquifers. The considerable amount of shale lithic fragments of medium grain size but containing large amounts of pelitic minerals may account for the inverse trend. Of course, it is not true that all medium-sand aquifers consist of shale lithic fragments. The second
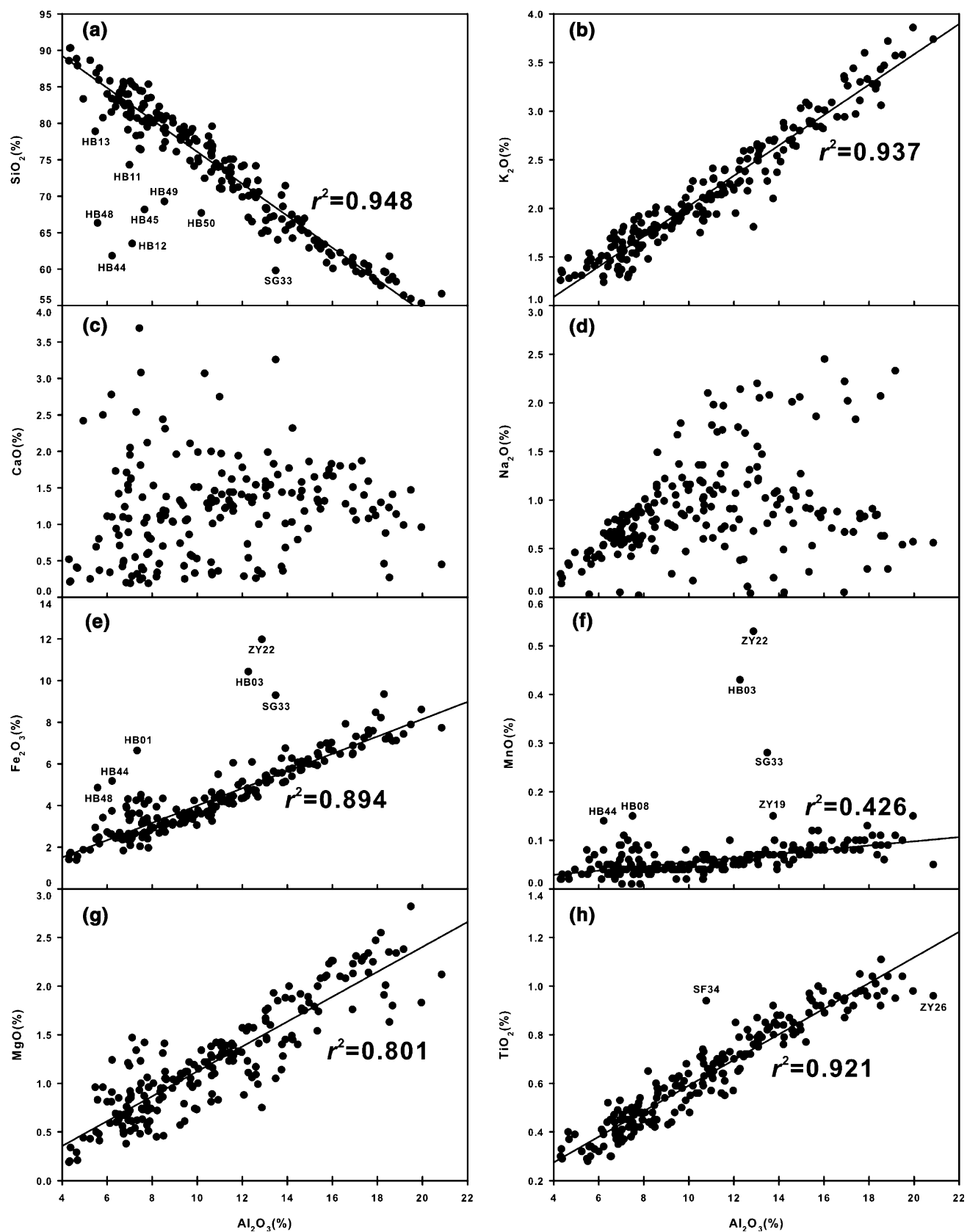
Table 1 MINLITH normative minerals

Mineral name	Abbreviation	Formula
Albite	Ab	$Na_2O \cdot Al_2O_3 \cdot 6SiO_2$
Anorthite	An	$CaO \cdot Al_2O_3 \cdot 2SiO_2$
Ankerite	Ank	$CaO \cdot FeO \cdot 2CO_2$
Apatite	Ap	$3CaO \cdot P_2O_5 + 1/3(CaF_2)$
Calcite	Cc	$CaO \cdot CO_2$
Chlorite	Chl	$k1MgO \cdot k2FeO \cdot k3Al_2O_3 \cdot k4SiO_2 \cdot 4H_2O$
Carbon	C	C
Dolomite	Dl	$CaO \cdot MgO \cdot 2CO_2$
Fluorite	Fl	CaF_2
Gibbsite	Gb	$Al_2O_3 \cdot 3H_2O$
Goethite	Gt	$Fe_2O_3 \cdot H_2O$
Gypsum	Gy	$CaO \cdot SO_3 \cdot 2H_2O$
Halite	Hl	$Na_2 \cdot 2Cl$
Hematite	Ht	Fe_2O_3
Illite	Ill	$2K_2O \cdot MgO \cdot FeO \cdot 6.5Al_2O_3 \cdot 16SiO_2 \cdot 5H_2O$[a]
Kaolinite	Kn	$Al_2O_3 \cdot 2SiO_2 \cdot 2H_2O$
Montmorillonite	Mm	$Na_2O \cdot 2MgO \cdot 5Al_2O_3 \cdot 24SiO_2 \cdot 6H_2O$
Magnesite	Mst	$MgO \cdot CO_2$
Orthoclase	Or	$K_2O \cdot Al_2O_3 \cdot 6SiO_2$
Pyrite	Py	FeS_2
Pyrolusite	Prl	MnO_2
Quartz	Q	SiO_2
Rhodochrosite	Rch	$MnO \cdot CO_2$
Rutile	Rt	TiO_2
Siderite	Sd	$FeO \cdot CO_2$
Serpentine	Srp	$3MgO \cdot 2SiO_2 \cdot 2H_2O$

[a] The values of $k1$, $k2$, $k3$ and $k4$ are weighting factors used in general chlorite formula (adapted from Rosena et al. 2004)

aquifer in site 4, a medium-sand aquifer, does not have a high content of pelitic minerals because the lithic fragments may be graywacke in origin. However, because of

the possibility of interference from lithic fragments on pelitic minerals during the estimation of hydraulic conductivity, medium-sand and coarser grained aquifers are not suitable for such measurement under this scheme.

Determination of hydraulic conductivity

The hydraulic conductivity obtained from conventional pumping test in this study represents an average value of the whole monitored aquifer. In contrast, XRF analysis gives chemical compositions for a single lithological layer as do the derived normative mineralogical compositions. To bring about correlation with aquifer hydraulic conductivity, normative mineralogical compositions are integrated through the whole aquifer based on stratigraphic columns. Table 2 shows the integral normative mineralogical compositions. As mentioned above, grain-size distribution and particle shape play a pivotal role in soil physical properties, e.g., hydraulic conductivity. Accordingly, normative minerals are characterized by their crystal shape. As shown in Table 3, the minerals are grouped into four categories: phyllosilicate, tectosilicate, earthy minerals and granular minerals. The categories of phyllosilicate and tectosilicate represent the most dominant altered and relic minerals, respectively. To include all accessory minerals with similar crystal shapes, the phyllosilicate and tectosilicate categorizations are expanded to include earthy and granular minerals, respectively. The amounts of these mineral categories in sampled aquifers are then calculated (Table 4). The hydraulic conductivities listed in Table 4 were determined by conventional single-well pumping test after well development and performance

Fig. 4 Plot of pelitic minerals versus tectosilicates. The labeled data, which are excluded from regression analysis, are samples deviating from the regression line due to the presence of iron nodules or calcareous fragments. The assemblages of pelitic minerals and tectosilicates are noted in the text
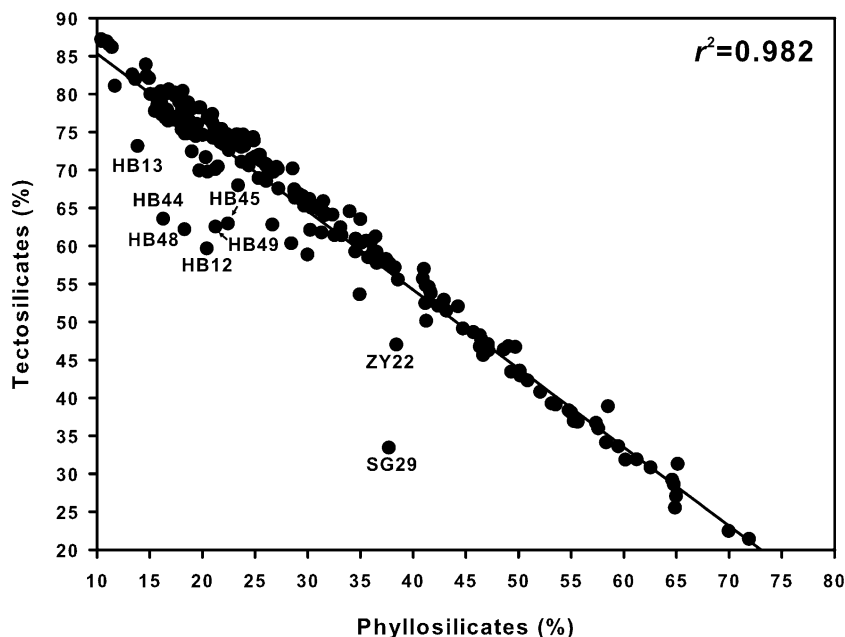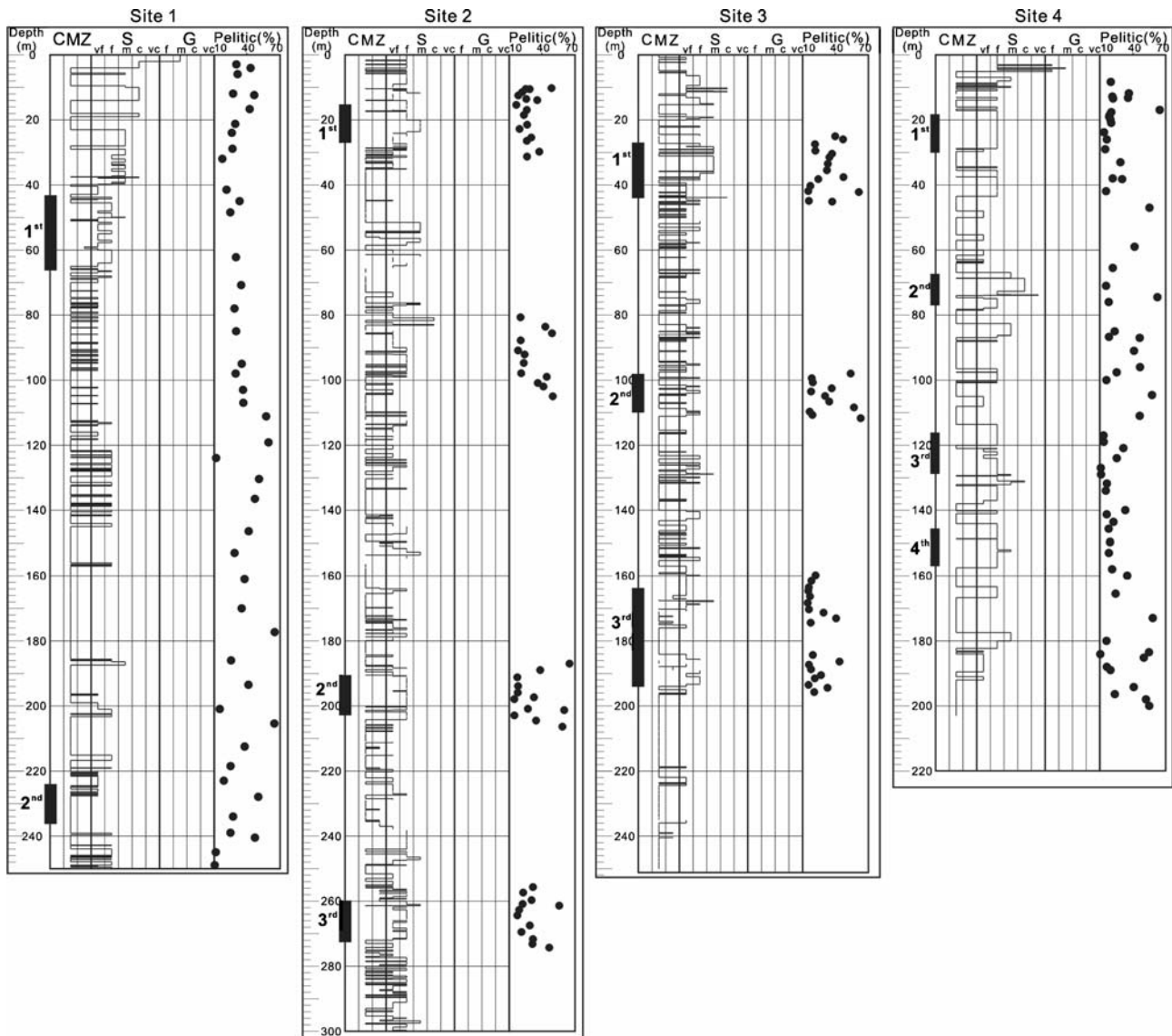
Fig. 5 Distribution of pelitic minerals (wt%) in depth and corresponding stratigraphic columns for the four sites

test. Whereas the sampled aquifers are all confined, pumping rate, well diameter and water-level drawdown with time were compiled to calculate transmissivities using the Jacob method (Cooper and Jacob 1946). Hydraulic conductivity values were subsequently determined by dividing the derived transmissivities by the saturated thickness of aquifer, and then correlated to corresponding selected mineral categories.

There are three medium-sand aquifers, which may contain considerable lithic fragments to violate the general relationship between grain size and mineralogical assemblage. These aquifers are excluded from the subsequent regression analysis on correlation with hydraulic conductivity. Figure 6 illustrates a linear log-

arithmic relationship of hydraulic conductivity (K in cm/s) to the concentration of mineral category (W in wt%). However, the earthy mineral and granular mineral should exactly play an opposite relationship because they are quantitatively complementary, and only category of earthy mineral is demonstrated. The best-fit equation is found as log $K = -1.292 - (0.0581 \times W_{\text{Earthy}})$ with the square of correlation coefficient (r^2) of 0.609 for nine sampled aquifers (Fig. 6c), which is of statistically low value but should be enough to quantitatively determine hydraulic conductivity in practice. The other two models of pelitic mineral and tectosilicate have slightly lower correlation coefficients (r^2s) of 0.58 (Fig. 6a) and 0.55 (Fig. 6b), respectively. This demonstrates that the normative mineral contents are effective to derive hydraulic conductivity as expected. In addition, the hydraulic conductivities of three medium-sand

Table 2 Integral normative mineralogical compositions for sampled aquifers in wt%

Normative minerals	Site 1		Site 2			Site 3			Site 4			
	First	Second	First	Second	Third	First	Second	Third	First	Second	Third	Fourth
Ab	10.84	7.95	14.01	5.35	7.52	4.96	5.42	6.15	3.82	3.17	2.79	4.54
An	1.15	0.84	1.49	0.57	0.80	0.53	0.48	0.65	0.40	0.34	0.29	0.48
Or	2.76	0.70	2.24	0.73	0.96	0.12	0.03	0.76	0.90	2.33	1.20	1.90
Q	51.90	55.54	51.07	65.96	60.65	54.82	53.70	65.03	69.05	59.81	74.25	62.31
Mm	0.00	3.20	0.20	2.03	2.99	6.25	6.09	1.88	0.00	2.96	0.01	0.00
Ill	20.93	23.14	19.57	19.28	17.64	22.96	21.48	17.33	14.19	17.08	15.89	12.33
Chl	7.90	4.66	6.73	2.46	5.66	4.61	4.49	3.76	2.58	8.53	2.29	6.83
Kn	0.00	0.00	0.00	0.00	0.00	0.06	2.89	0.00	0.00	0.80	0.13	0.00
Ap	0.28	0.24	0.29	0.22	0.28	0.27	0.33	0.24	0.18	0.22	0.14	0.24
Cc	1.31	0.00	0.66	0.10	0.59	0.26	0.00	0.82	4.40	1.87	0.04	5.55
Dl	0.14	0.26	0.87	0.15	0.00	0.65	0.06	0.53	1.07	0.08	0.44	0.84
Ank	1.83	1.46	1.17	1.24	2.07	3.27	0.47	1.51	2.05	1.74	0.88	4.43
Rch	0.09	0.00	0.06	0.01	0.06	0.03	0.00	0.04	0.07	0.07	0.03	0.14
Sd	0.00	0.00	0.00	0.00	0.00	0.01	0.00	0.00	0.00	0.00	0.00	0.00
Srp	0.03	0.03	0.08	0.17	0.00	0.00	0.07	0.05	0.06	0.00	0.00	0.00
Ht	0.17	1.20	0.89	1.16	0.16	0.56	3.54	0.68	0.86	0.40	1.19	0.00
Prl	0.00	0.05	0.02	0.04	0.01	0.04	0.17	0.03	0.02	0.05	0.03	0.00
Rt	0.67	0.73	0.65	0.53	0.61	0.60	0.78	0.54	0.35	0.55	0.40	0.41
Total	100.0	100.0	100.0	100.0	100.0	100.0	100.0	100.0	100.0	100.0	100.0	100.0

Table 3 Four categories of minerals based on crystal shape for subsequent correlation with hydraulic conductivity

| Normative minerals	Crystal shape	Category	
Mm	Earthy	Phyllosilicate	Earthy mineral
Ill	Earthy	Phyllosilicate	Earthy mineral
Chl	Platy	Phyllosilicate	Earthy mineral
Kn	Earthy	Phyllosilicate	Earthy mineral
Srp	Earthy, fibrous	Phyllosilicate	Earthy mineral
Prl	Earthy	Phyllosilicate	Earthy mineral
Q	Blocky	Tectosilicate	Granular mineral
Ab	Granular	Tectosilicate	Granular mineral
An	Granular	Tectosilicate	Granular mineral
Or	Blocky	Tectosilicate	Granular mineral
Ap	Granular		Granular mineral
Cc	Tabular		Granular mineral
Dl	Blocky		Granular mineral
Ank	Granular		Granular mineral
Rch	Granular		Granular mineral
Sd	Tabular		Granular mineral
Ht	Blocky		Granular mineral
Rt	Granular		Granular mineral

aquifers are highly underestimated based on the regression equations due to the aforementioned interference from shale lithic fragments as shown in Fig. 6. In contrast, the same regression analysis was conducted to examine whether there are linear logarithmic functions of hydraulic conductivity to SiO_2 and Al_2O_3 contents. Figure 7 illustrates that the correlation coefficients (r^2s) are all under 0.4, and not only does it confirm the ability of MINLITH algorithm in this kind of studies but also improves that crystal size and shape are the major factors to determine hydraulic conductivity.

Practically, conventional pumping tests have difficulty in measuring the hydraulic conductivity of poor conductive layers. Using the present method, there are advantages to applying a linear regression equation to the clayey layer. However, when the content of earthy minerals is extrapolated to 80%, hydraulic conductivity of 1.15×10^{-6} cm/s is obtained. In the absence of test data, this result is thought to overestimate the hydraulic conductivity, which should be less than 10^{-7} cm/s (Davis 1969). Such an error from extrapolating the best-fit

Table 4 The amounts of four mineral categories and corresponding aquifer hydraulic conductivities

Categories	Site 1		Site 2			Site 3			Site 4			
	First	Second	First	Second	Third	First	Second	Third	First	Second	Third	Fourth
Phyllosilicate (%)	28.83	30.99	26.51	23.78	26.29	33.88	34.95	22.98	16.77	29.38	18.31	19.16
Tectosilicate (%)	66.65	65.03	68.81	72.61	69.92	60.43	59.63	72.59	74.17	65.65	78.54	69.23
Earthy mineral (%)	30.86	33.73	28.66	26.38	28.53	37.75	39.20	25.24	19.74	31.57	20.41	23.59
Granular mineral (%)	69.14	66.27	71.34	73.62	71.47	62.25	60.80	74.76	80.26	68.43	79.59	76.41
Hydraulic conductivity ($\times 10^{-4}$ cm/s)	12.4	15.8	93.3	16.1	5.81	117.0	1.94	17.7	41.7	33.5	46.2	17.1

Fig. 6 Plots of concentration of each mineral category versus hydraulic conductivity. The category of granular minerals is not shown here due to its exact opposite relationship with earthy minerals. The labeled data (*solid square*) are excluded from the regression analysis due to substantial lithic fragments
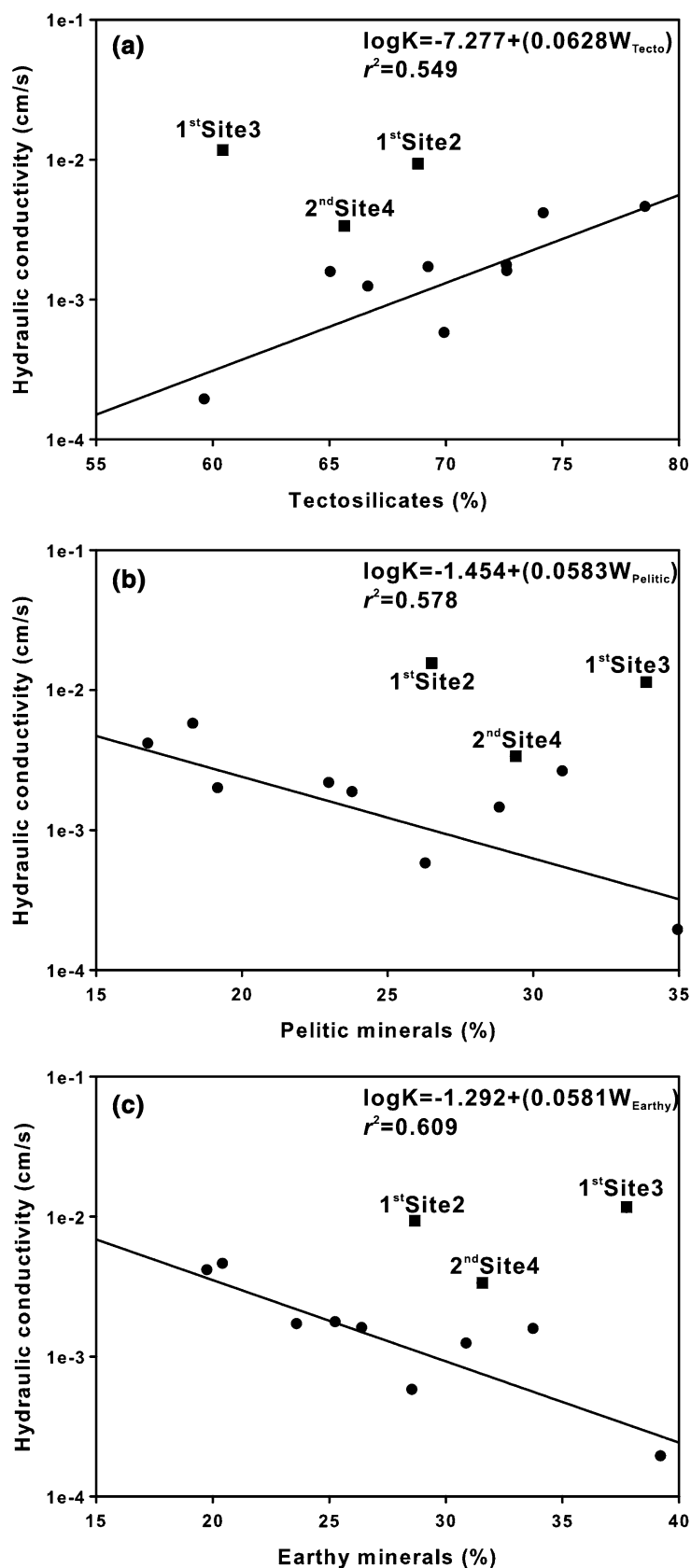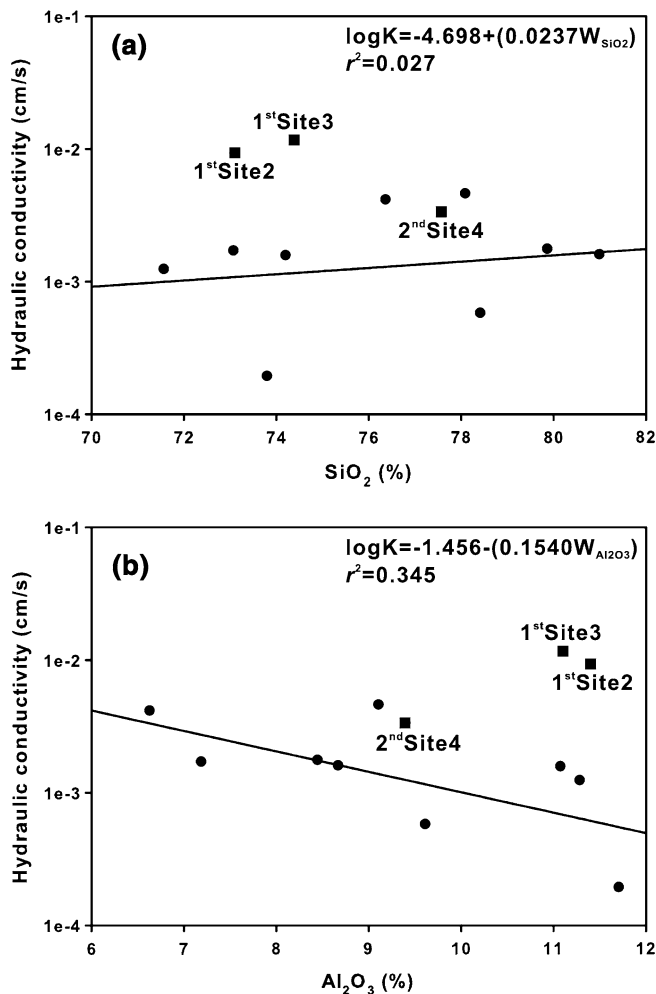
Fig. 7 Plots of concentrations of SiO_2 and Al_2O_3 versus hydraulic conductivity. The labeled (*solid square*) data are not included in the regression analysis for the same reason as Fig. 6

equation may possibly be caused by ignoring the effect of soil compaction in this study. Generally, clayey layer has higher degree of compaction; as a result, the hydraulic conductivity may dramatically decrease with increasing earthy minerals. As mentioned in Introduction, the slug test in direct-push drilling method and dipole-flow test are useful to provide a higher resolution about spatial variations in hydraulic conductivity. To correlate more data from these profiling tests with sediment geochemical compositions may overcome the difficulty in overestimating hydraulic conductivity of clayey layer. On the contrary, the relationship developed in this study is a good supplement to the unscreened interval of a well where profiling tests cannot be conducted along.

Conclusions

1. Sampled aquifers are mainly composed of phyllosilicates and quartz with calcareous fossils or iron nodules being the major mechanisms modifying geochemical characteristics inherited from parent rocks. Therefore, most of the samples contain minor unstable minerals, for instance the pyroxene and olivine. These characters were used to determine suitable for MINLITH algorithm analysis to derive normative mineralogical compositions.
2. The normative mineralogical compositions calculated by the MINLITH algorithm do not violate conclusions based on geochemical characteristics. Validation of the MINLITH computer code is approved and the derived normative minerals are representative of the quantitatively significant components of genuine mineralogical assemblages.
3. The hydraulic conductivities of the sampled aquifers do not show a definite relationship with elemental contents. After the conversion from bulk chemical compositions to normative mineralogical assemblages using the MINLITH algorithm, the hydraulic conductivity (K in cm/s) can be expressed as a linear logarithmic equation to earthy mineral content (W_{earthy} in wt%): $\log K = -1.292 - (0.0581 \times W_{Earthy})$. Accordingly, crystal size and shape are major factors determining hydraulic conductivity.
4. The linear regression equation mentioned above is only applicable in the determination of hydraulic conductivity for fine-sand, silty and clayey layers. The layers with coarser grain size may contain considerable lithic fragments, which interfere with the relationship between geochemical characteristics and grain-size distribution. In addition, this equation tends to overestimate hydraulic conductivity by one order if the content of earthy minerals is extrapolated to 80%.

References

Butler JJ Jr, Healey JM, McCall GW, Garnett EJ, Loheide SP II (2002) Hydraulic tests with direct push equipment. Ground Water 40(1):25–36

de Caritat P, Bloch J, Hutcheon I (1994) LPNORM: a linear programming normative analysis code. Comput Geosci 20(3):313–347

Cohen D, Ward CR (1991) SEDNORM—a program to calculate a normative mineralogy for sedimentary rocks based on chemical analyses. Comput Geosci 17(9):1235–1253

Cooper HH, Jacob CE (1946) A generalized graphical method for evaluating formation constants and summarizing well field history. Am Geophys Union Trans 27:526–534

Croft MG (1971) A method of calculating permeability from electric logs. U.S. Geol Surv Prof Pap 750-B:B265–B269

Cross W, Iddings JP, Pirsson LV, Washington HS (1902) A quantitative chemico-mineralogical classification and nomenclature of igneous rocks. J Geol 10:555–690

Currie KL (1991) GENORM: a generalized norm calculation. Comput Geosci 17(1):77–89

Davis SN (1969) Porosity and permeability of natural materials. In: De Wuest RJM (eds) Flow through porous media. Academic, New York, pp. 54–89

Davis ROE, Bennett HH (1927) Grouping of soils on the basis of mechanical analysis. United States Department of Agriculture Departmental Circulation No. 419

Gaur RS, Singh I (1965) Relation between permeability and gamma-ray intensity for the Oligocene sand of an Indian field, India (Republic). Oil Nat Gas Comm Bull 2:74–77

Hazen A (1911) Discussion of 'Dams on sand foundations'. Trans Am Soc Civ Eng 73:199

Hinsby K, Bjerg PL, Andersen LJ, Skov B, Clausen EV (1992) A mini slug test method for determination of a local hydraulic conductivity of an unconfined sandy aquifer. J Hydrol 136:87–106

Holail HM, Moghazi AKM (1998) Provenance, tectonic setting and geochemistry of greywackes and siltstones of the Late Precambrian Hammamat Group, Egypt. Sediment Geol 116:227–250

Kabala ZJ (1993) The dipole flow test: a new single-borehole test for aquifer characterization. Water Resour Res 29(1):99–107

Merodio JC, Spalletti LA, Bertone LM (1992) A FORTRAN program for the calculation of normative composition of clay minerals and pelitic rocks. Comput Geosci 18(1):47–61

Paktunc AD (1998) MODAN: an interactive computer program for estimating mineral quantities based on bulk composition. Comput Geosci 24(5):425–431

Pryor WA (1973) Permeability-porosity patterns and variations in some Holocene sand bodies. Am Assoc Pet Geol Bull 57(1):162–189

Rabe CL (1957) A relation between gamma radiation and permeability, Denver–Julesburg basin. Trans Soc Pet Eng Am Inst Mining, Metallurg Pet Eng 210:358–360

Rosena OM, Abbyasovb AA, Tipperc JC (2004) MINLITH—an experience-based algorithm for estimating the likely mineralogical compositions of sedimentary rocks from bulk chemical analyses. Comput Geosci 30(6):647–661

Shepherd RG (1989) Correlations of permeability and grain size. Ground Water 27(5):633–639

Wentworth CK (1922) A scale of grade and class terms of clastic sediments. J Geol 30:377–392

Zlotnik VA, Ledder G (1996) Theory of dipole flow in uniform anisotropic aquifers. Water Resour Res 32(4):1119–1128